Hindawi
Advances in Civil Engineering
Volume 2019, Article ID 9743295, 9 pages
https://doi.org/10.1155/2019/9743295

Research Article

Method Improvements of Testing Modulus of Soil Based on Free-Vibration Column

Dandan Jin[1], **Xianwen Huang**[2,3], **Binghui Wang**[3], **Aizhao Zhou**[3] and **Shunqing Liu**[3]

[1]*Faculty of Civil Engineering and Mechanics, Jiangsu University, Zhenjiang, Jiangsu 212013, China*
[2]*School of Architecture and Civil Engineering, Anhui University of Science and Technology, Fanjian Road, Huainan, Anhui 232001, China*
[3]*School of Architecture and Civil Engineering, Jiangsu University of Science and Technology, Zhenjiang, Jiangsu 212000, China*

Correspondence should be addressed to Binghui Wang; wbhchina@126.com

Received 22 June 2019; Accepted 8 October 2019; Published 31 October 2019

Academic Editor: Paolo Castaldo

It is difficult to directly measure the dynamic elastic modulus of soils when the strain is less than 10^{-4}, though the dynamic shear modulus can be easily obtained by the free-vibration testing method. Some improvements were adapted to the traditional free-vibration column for measuring dynamic elastic modulus of soil precisely with lateral vibration in small strain (10^{-4}~10^{-6}). Differing from the traditional lateral vibration theory, a new dynamic elastic modulus testing method based on bending vibration equation of cantilever beam was put forward based on the improved free-vibration column of GZZ-50. Firstly, some descriptions about calibration process of needed testing parameter (moment of inertia of drive board) were made, and then, Poisson's ratio of standardized column was used to confirm the measured results. Four main improvements were applied, including the shape of drive board which made the bending vibration equation solved, laser displacement sensors for correcting specimen's height parameter with uncontacted manner which can reduce the influence of specimen, a hoop with plug used to make the split mould be removed, and air duct used when installing drive board to increase the success rate of installing specimen. Finally, standard process of installing specimen was described, which can be used as reference of similar test.

1. Introduction

In recent years, more and more attention was paid to near-field earthquake, and the dynamic characteristic of soil under the effect of vertical earthquake was being more important in earthquake engineering. There are many indoor testing methods which were utilized to measure dynamic parameters of soil, such as the wave velocity method of bending element [1], resonant column [2] or free-vibration column testing method [3], dynamic triaxial testing method [4, 5], shear vibration testing method (torsion in the hollow column) [6, 7], and (centrifugal) shaking table test method [8, 9]. With the development of science and technology in testing instruments and increasing requirements of dynamic parameters of soil, testing instruments of dynamic characteristic of soil have been improving [10, 11]. Many new testing functions had been added [12], and more comprehensive testing theory had been put forward [13, 14].

In soil dynamics and earthquake engineering, the dynamic shear and elastic modulus are the basic dynamic parameters of soil [15]. Dynamic triaxial test [16] is recognized as the most suitable instrument to measure the dynamic elastic modulus of soil, whose test results are reliable when the dynamic strain is between 10^{-4} and 10^{-2}. But, the testing results are controversial when the strain is smaller than 10^{-4} due to the accuracy effect of testing instrument. When dynamic strain is smaller than 10^{-4}, dynamic elastic or shear modulus of soil can be measured accurately by resonant (free-vibration) column in theory. The results of dynamic shear modulus measured by resonant (free-vibration) column with torsion in small strain is accepted by researchers [2, 3], and the testing process is simple, but the

dynamic elastic modulus of soil is hard to be measured through axial vibrating of resonant (free-vibration) column, and less progress appears in this area decades.

Cascante et al. [17] put forward a theory that the lateral vibration equation of cantilever beam can be used to measure the dynamic elastic modulus of soil simply. The lateral vibration of soil column was presumed as cubic polynomial equation, and the energy method and material mechanics were utilized to solve the frequency equation of bending vibration. Based on Cascabte's method, Madhusudhan et al. [18] obtained the dynamic elastic modulus of Bangalore sand from lateral vibration tests. Analyzing the testing and solution process of the dynamic elastic modulus of Bangalore sand, the reasonability of some assumes is doubtful, such as the effect of bending moment of the drive board whether can be ignored and the vibration shape of soil column whether is reasonable. All of these will lead to deviation of testing results. In this paper, a new testing method to measure dynamic elastic modulus in presume that soil is elastic materials in small strain ($<10^{-4}$) was put forward, whose reasonability had been proved [19]. The new method based on bending vibration equation [20] can consider the shear force and bending moment of the drive board well at the same time and remove the presume of cubic polynomial equation on vibration shape. Wang et al. [21] had discussed the solution process of this method and put forward that it can be applied to measure measuring dynamic elastic modulus of soil. But, they did not combine the corresponding instruments to describe the bending vibration equation detailed and did not explain the reasonability of some boundary conditions.

Based on the above analysis, the article detailed the solution process of dynamic elastic modulus of soil column in terms of bending vibration equation and made four main improvements of traditional free-vibration column, which expands the testing scope of soil that cannot keep stability of the fixed shape in common confining pressure and improves the testing result quality of the specimen. The simple instruction of the instrument in this paper is shown in Figure 1, (see the Appendix part of this paper). For better using improved GZZ-50 free-vibration column (made in china), the calibration process of the needed testing parameter (moment of inertia of the drive board) and the installation process of the specimen were detailed, and the deal processing of data was described briefly.

2. Dynamic Elastic Modulus Testing Theory

2.1. Bending Vibration Equation. Cascante et al. [17] earlier put forward the appliance of lateral vibration test method in measuring the dynamic elastic modulus of soil. In analyzing, the vibration shape of soil column is assumed as cubic polynomial equation, and the additional force of drive board to the top of soil column is recognized as vertical shear force F. Then, material mechanics and energy method were used to solve the bending vibration equation. In Cascante's method, there are two main purposes: Firstly, the vibration

Figure 1: Introduction of free-vibration column of GZZ-50.

shape of soil column is defined as cubic polynomial equation, whose reliability is not sure. Secondly, when vibrating, the effect of drive board to the top of soil column is assumed as shear force, which ignores the effect of bending moment of the drive board. In real structure, the additional bending moment of the drive board is large, which has significant influence of the bending of soil column, and the influence will be more obvious with increasing strain. So, it is meaningful to find a more comprehensive method to calculate the dynamic elastic modulus of soil.

Bending vibration equation of cantilever beam with additional mass is a good solution to calculate dynamic elastic modulus of uniform materials, and the corresponding calculating model is shown in Figure 2. When calculating, the drive board is assumed as an additional mass attached at the top of beam, and the effect of additional mass to the top of soil column is recognized as shear force and bending moment according to the position of drive board (shown in Figure 3). For solving the frequency equation, some considerations were put forward including ① the strain of soil is in elastic period; ② some basic physical parameters of specimen are known or obtained, such as the diameter D, height L, mass m, and antibending stiffness EI; and ③ the mass and rotate inertia of the drive board m_t and J_t have been measured or achieved.

The microelement diagram of cantilever beam in lateral vibration is shown in Figure 4. Rao [20] set up the bending vibration equation of cantilever beam with additional mass $y(x,t)$ according to the force characteristic of cantilever beam with additional mass, which is shown in

$$EI\frac{\partial^4 y}{\partial x^4} + \rho S\frac{\partial^2 y}{\partial t^2} = f(x,t) - \frac{\partial}{\partial x}m(x,t). \tag{1}$$

In actual testing, the exciting force which is arisen from the drive board makes the specimen obtain an initial strain in the specimen and then disappears quickly. After that, the specimen will vibrate in natural frequency and the vibrating amplitude will reduce gradually under the effect of damping. So, in solution process of free-vibration equation, the additional exciting force in function 1 is set as zero, and the free-vibration equation will be simplified to

$$\frac{\partial^2}{\partial x^2}\left[EI\frac{\partial^2 y(x,t)}{\partial x^2}\right] + \rho S\frac{\partial^2 y(x,t)}{\partial t^2} = 0. \tag{2}$$

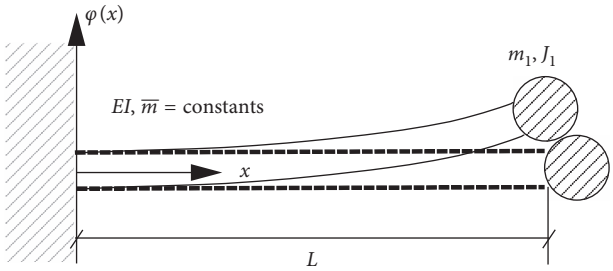

Figure 2: Vibration model of cantilever beam with additional mass.

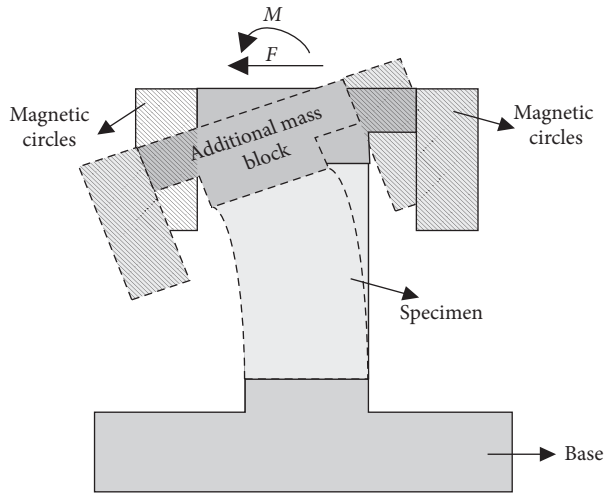

Figure 3: Model of lateral vibration with drive board.

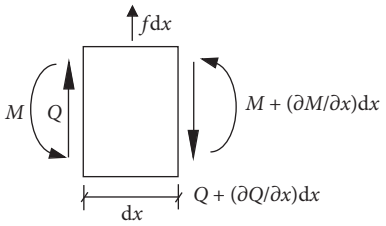

Figure 4: Microelement diagram of cantilever beam.

2.2. Solution of Dynamic Elastic Modulus. Function 2 can be solved using separation variable method and will be separated to

$$\begin{cases} Y(t) = B_1 \sin(\omega t) + B_2 \cos(\omega t), \\ \phi(x) = A_1 \cos\beta x + A_2 \sin\beta x + A_3 \mathrm{ch}\beta x + A_4 \mathrm{sh}\beta x, \end{cases} \tag{3}$$

where ω is the natural frequency, B_1 and B_2 are constants which can be confirmed according to initial situation, A_1, A_2, A_3, and A_4 are constants, which can be achieved from boundary conditions, and β can be repeated by $\beta^4 = \overline{m}\omega^2/EI$ where $\overline{m}$ is mass per length of cantilever beam.

Based on the boundary conditions from the fixed end of cantilever beam, function (4) can be obtained:

$$\begin{cases} \phi(x) = 0, \\ \phi'(x) = 0. \end{cases} \tag{4}$$

The function (5) can be achieved by combining function 3 and 4

$$\begin{cases} A_3 = -A_1, \\ A_4 = -A_2. \end{cases} \tag{5}$$

When vibrating, the shear force which is arisen from the drive board can be represented as $V(L) = -\omega^2\phi(L)m_t$, where m_t is the mass of the drive board. Also, the bending moment which arises from rotation of the drive board can be represented as $M(L) = -[\omega^2\phi'(L)J_t + m_t d_0^2]$. J_t is the rotary mass moment of inertia of the drive board. The corresponding boundary conditions can be achieved in

$$\begin{cases} EI\phi''(L) = -\left[\omega^2\phi'(L)J_t + m_t d_0^2\right], \\ EI\phi'''(L) = -\omega^2\phi(L)m_t, \end{cases} \tag{6}$$

where $d_0 = 0$ can be obtained if the rotate axis of the drive board is set at the top of cantilever beam, which will be described in detail in Section 3.1. Combining functions (3), (5), and (6), function (7) can be obtained:

$$\begin{bmatrix} \beta^2(\cos\beta L + \mathrm{ch}\beta L) - \dfrac{\omega^2 J_t}{EI}\beta(\sin\beta L + \mathrm{sh}\beta L) & \beta^2(\sin\beta L + \mathrm{sh}\beta L) + \dfrac{\omega^2 J_t}{EI}\beta(\cos\beta L - \mathrm{ch}\beta L) \\ \beta^3(\sin\beta L - \mathrm{sh}\beta L) + \dfrac{\omega^2 m_t}{EI}(\cos\beta L - \mathrm{ch}\beta L) & -\beta^3(\cos\beta L + \mathrm{ch}\beta L) + \dfrac{\omega^2 m_t}{EI}(\sin\beta L - \mathrm{sh}\beta L) \end{bmatrix} \begin{Bmatrix} A_1 \\ A_2 \end{Bmatrix} = \begin{Bmatrix} 0 \\ 0 \end{Bmatrix}. \quad (7)$$

Function (7) is meaningful, and A_1 and A_2 are nonzero, so function (8) can be obtained:

$$\begin{aligned} &\left[\beta^2(\cos\beta L + \mathrm{ch}\beta L) - \frac{\omega^2 J_t}{EI}\beta(\sin\beta L + \mathrm{sh}\beta L)\right] \\ &\cdot\left[-\beta^3(\cos\beta L + \mathrm{ch}\beta L) + \frac{\omega^2 m_t}{EI}(\sin\beta L - \mathrm{sh}\beta L)\right] \\ &-\left[\beta^2(\sin\beta L + \mathrm{sh}\beta L) + \frac{\omega^2 J_t}{EI}\beta(\cos\beta L - \mathrm{ch}\beta L)\right] \\ &\cdot\left[\beta^3(\sin\beta L - \mathrm{sh}\beta L) + \frac{\omega^2 m_t}{EI}(\cos\beta L - \mathrm{ch}\beta L)\right] = 0, \end{aligned} \quad (8)$$

where $z \equiv \beta L$ and $\beta^4 = \overline{m}\omega^2/EI$ can be used to simplify function 8, and function 9 can be obtained:

$$\begin{aligned} &\alpha_J\alpha_m z^4(1 - \cos z\mathrm{ch}z) + \alpha_m z(\sin z\mathrm{ch}z - \cos z\mathrm{sh}z) \\ &\quad = \alpha_J z^3(\sin z\mathrm{ch}z + \cos z\mathrm{sh}z) + (1 + \cos z\mathrm{ch}z), \end{aligned} \quad (9)$$

where $\alpha_J = (J_t/\overline{m}L^3) = (J_t/mL^2)$ and $\alpha_m = (m_t/\overline{m}L) = (m_t/m)$. α_J and α_m are two dimensionless parameters which have concrete physical meaning. α_J is the rotate inertia ratio between the drive board and specimen column which can be obtained by calibrating and calculating (described in Section 2.1), and α_m is the mass ratio between the drive board and specimen which can be obtained by weighting directly.

It is hard to acquire the value of z directly in function 9, for it is a transcendental equation. Hence, the numerical solution can be chosen to calculate the value of z. And then, the dynamic elastic modulus E can be achieved as shown in

$$E = \frac{m_t\omega^2 L^3}{z^4 I}. \quad (10)$$

3. The Calibration of System Parameters

3.1. Testing Process of Calibration. Before calibrating the testing parameters, some basic information about specimen is needed, including: the height L, diameter D, mass m, and the mass of the drive board m_t. The calibrating parameter J_t is hard to be measured directly for the complicated shape of drive board. When calibrating, more than 3 standard bars whose heights are different are needed, and they are made of identical materials and have the same section size, but the heights of them are different. The installed standard bar (shown in Figure 5) and concrete testing process are shown in the following:

① Make some measurements about needed parameters, including the height and mass of two standard bars L_1, L_2, m_1, and m_2 and the mass of drive board m_t, and calculate the moment of inertia of the standard bar I_b.

② Separately conduct the tests of bending vibration of two standard bars. Then, the natural frequencies ω_1 and ω_2 of them can be obtained with the accelerometers according to different heights of standard bars.

③ Solve function 9 which includes two unknown parameters J_t and E in the method of combining two different equations, and the corresponding dynamic elastic modulus of standard bar E and rotational inertia of the drive board J_t can be obtained;

④ Repeat the process ② and ③ and calculate the E and J_t many times to reduce the mistakes arisen from the data collection and calculation.

⑤ Select different heights of standard bar, and repeat the above process. J_t can be corrected gradually to reduce the effect of standard bars' height to the testing results.

3.2. Checking with Standard Bar. After the rotational inertia of the drive board J_t is obtained, it is meaningful to check the measured results of free-vibration column. So, the standard bar consisted of elastic material, whose Poisson' ratio is known can be used to check the measured results. The testing results are shown in Figures 6 and 7 separately.

As is shown in Figure 6, it can be found that dynamic shear modulus reduces less with the increase of dynamic strain. The average dynamic shear modulus is 75.84 GPa, and the difference between the maximum and minimum is 1.5%, which met the requirements of tests. The same changing tendency appears in the dynamic elastic modulus. The maximum dynamic elastic modulus 190.20 GPa appears at strain 2.35×10^{-6}, the minimum value 187.92 GPa appears at strain 4.48×10^{-5}, and the difference between them is 1.2% which met the requirements of tests. Based on the test results of elastic modulus, it can be found that the lateral vibration test has a good testing result in measuring the elastic modulus.

Comparing the average dynamic elastic modulus and shear modulus, considering the Hooke's law which describes the relationship between elastic modulus and shear modulus, Poisson's ratio of material μ can be obtained according to $G = E/2(1 + \mu)$. Poisson's ratio of the standard bar is 0.244, which is included in the period between 0.24 and 0.25. Poisson's ratio of the standard bar can be obtained from manufacturers. Poisson's ratio is connected with materials,

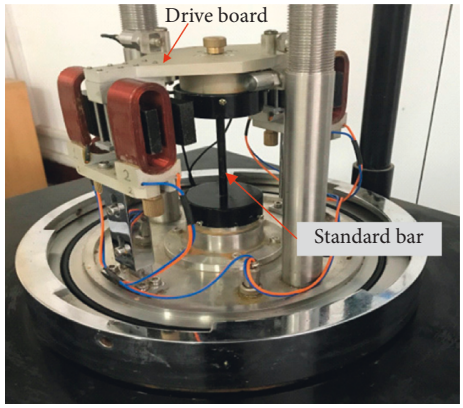

Figure 5: Photo of installed standard bar.

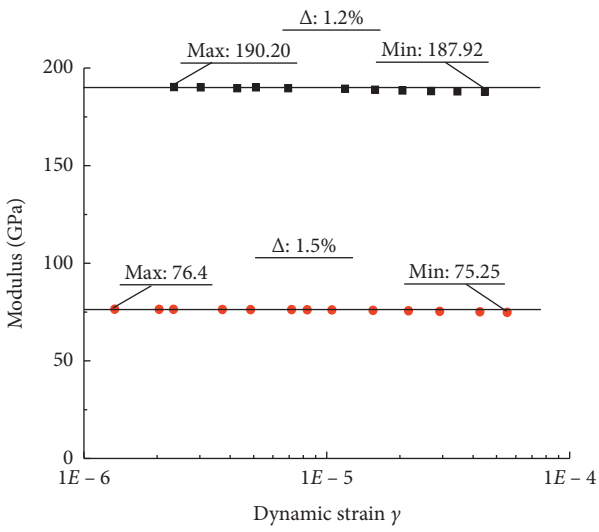

Figure 6: Test results of modulus.

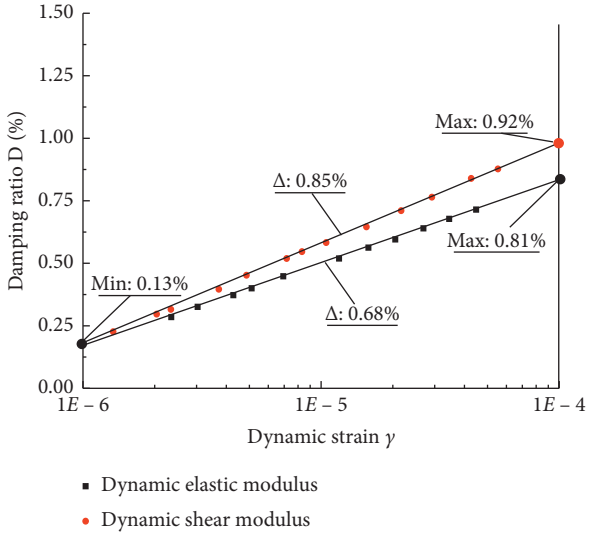

Figure 7: Test results of damping ratio.

which is easy to be obtained in real. So, it can be easily used to check the testing results.

Figure 7 shows the damping ratio and strain. It can be found that the damping ratio increases with the increasing of strain in lateral and shear vibrating tests, but the relative errors of damping ratio 0.85% and 0.68% are less than the requirements (2%). It means that the lateral and shear vibrating tests have a good result of the damping ratio by the improved instrument in this paper.

4. Discussion about Improved Instrument

4.1. Adjustment of Drive Board Shape. As is shown in Figures 8 and 9, it can be found that greater difference appears at the relative position of drive device (magnets) in the drive board. In traditional resonant column (shown in Figure 8), the drive device is set at the middle height of the drive board, which means that the mass center is in the middle of the drive board. In improved instrument, the drive device is set at the bottom height of the drive board, which means the mass center can be controlled at the bottom of the drive board in the method of attaching additional mass.

When calculating the additional bending moment of the drive board, it is necessary to confirm the displacement between the drive board and the top of specimen column. The displacement reflects the value of d_0 in function 6. It is hard to measure the height of the mass center of the drive board to the top of specimen in traditional resonant column, but the problem can be solved well through the movement of the magnets' position, which made the mass center be limited at the bottom of the drive board. So, the value of d_0 in function 6 can be set as zero.

4.2. Installation of Laser Displacement Sensors. In experiments, the height of specimen will reduce during the necessary process of consolidation before vibrating; especially, the reduced height of specimen is more obvious when the specimen is soft soil. If we ignore it, then greater errors will appear. The effects of relative errors of specimen's height to calculating results are shown in Table 1:

As shown in Table 1, due to the height changes of specimen, calculation relative errors will appear and increase rapidly with the increasing of measured height changes of specimen. When the relative error of height is 1 mm, the relative calculation errors will arrive at 2.97%, which is over the allowable error of tests (2%), and the calculation relative errors will increase rapidly with the increasing of height errors under the effect of cubed L in Function 10. So, it is significant to continuously confirm the height of specimen. In improved instruments, the laser displacement sensor was set above drive board, with a reflective face using a flat top screw installed at the center of the drive board (shown in Figure 10).

5. The Installation Process of Specimen

5.1. The Detailed Installation Process. For better application of improved resonant (free-vibration) column, authors described the installation process standardly, which is shown in the following steps:

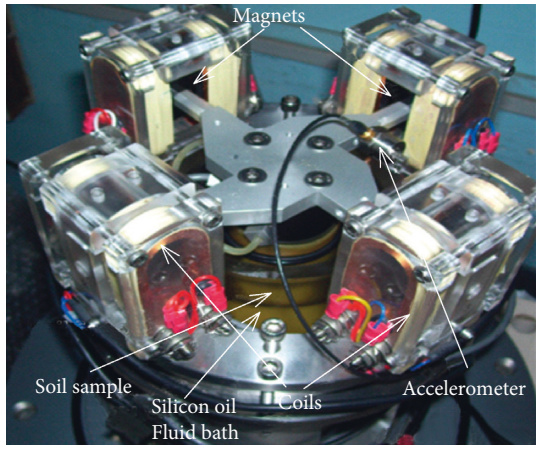

Figure 8: Photo of traditional resonant column (copy from Madhusudhan and Senetakis [18]).

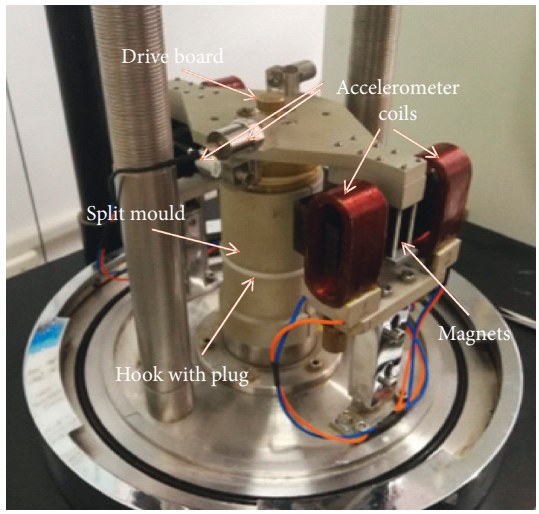

Figure 9: Photo of free-vibration column of GZZ-50.

① Soil column with height 100 mm and diameter 50 mm is prepared, and the weight of it has been measured. The prepared specimen should be kept constant. The filter paper should be put at the double end of soil column (shown in Figure 11), which can not only avoid the block of water-permeable stone but also can reduce the partial destruction of stress arisen from the blade of the drive board when vibrating.

② Installation of the split mould is important for some low-strength soils which cannot retain the shape in natural pressure. The plug embeds the hoop with two circles, which can fix the split mould as shown in Figure 12. The rubber diaphragm was turned down, and the rubber band was set.

③ Set the drive board, connect the accelerometers, turn up the rubber diaphragm, move up the rubber band, and install the electromagnetic coil. It is important in this period that the blade of the drive board did not embed the soil.

④ Push down the drive board vertically till the designed position and avoid rotating. The air focused on the top of specimen will remove along the hollow duct. After that, the hollow duct will be moved out.

⑤ Set the two lines to the designed line ring which can be hooked when testing (shown in Figure 10). Then, set confining pressure.

⑥ Rotate the control bar to pull out the plug and open the split mould separately horizontally (shown in Figures 10 and 13). Then, the installation of specimen has been finished.

5.2. Addition of Hoop with Plug. It is a bigger problem for resonant (free-vibration) column to measure the dynamic characteristic of soft soil, such as soft clay or loose sand. When testing, the specimen probably collapses under the gravity force of the drive board without effective confining pressure or the split mould supporting, which will lead to bad testing results or even failure of tests. Also, if the effective confining pressure exists, specimen can keep the original shape of the specimen without the split mould supporting in many cases. So, it is meaningful to remove the support of split mould without releasing the effective confining pressure in experiment.

Hence, the hoop with plug (shown in Figure 12) was added, which can simply make the split mould be removed without releasing confining pressure. The plug can be pulled out by the hook setting at the top of the device, and the constraint of split mould to the specimen will disappear. Then, the two split moulds will open (shown in Figure 13) under the effect of leash controlled by the hook too. The abovementioned device allowed the split mould to be removed under confining pressure, and owing to this improvement, the system expands the testing scope of soil types.

5.3. Addition of Air Duct. The contacting quality of the drive board to the soil column will have great influence to the testing results of specimen, but it is hard to guarantee in real installation. The contacting quality is closely related to the blade embed effect. When installing rubber diaphragm, rubber band, and other devices, it is significant to reduce disturbance of contacts between the drive board and specimen. In low-permeability materials, when the drive board was pushed down vertically, the air which is focused on void between the top of specimen and the drive board will be compressed. It will rebound the drive board after removing the push force, which will reduce the contacting quality seriously. So, the hollow duct can be used (shown in Figure 14) to solve the problem through removing the air focused on the top of specimen. After installation, due to the effect of lubricating oil attached on the duct, the duct will be removed in low-disturbing level.

Table 1: The relative errors of height changes.

Relative errors of height (mm)	1	2	3	4	5	6	7	8	9
Calculation relative errors (%)	2.97	5.88	8.73	11.52	14.26	16.94	19.56	22.13	24.64

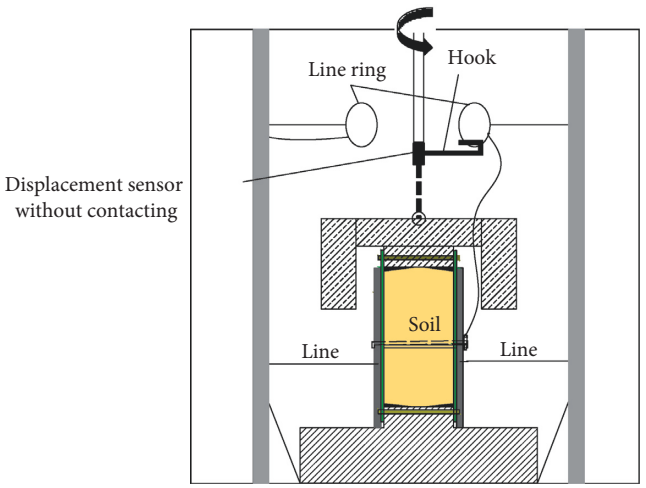

Figure 10: Schematic diagram of process ⑤.

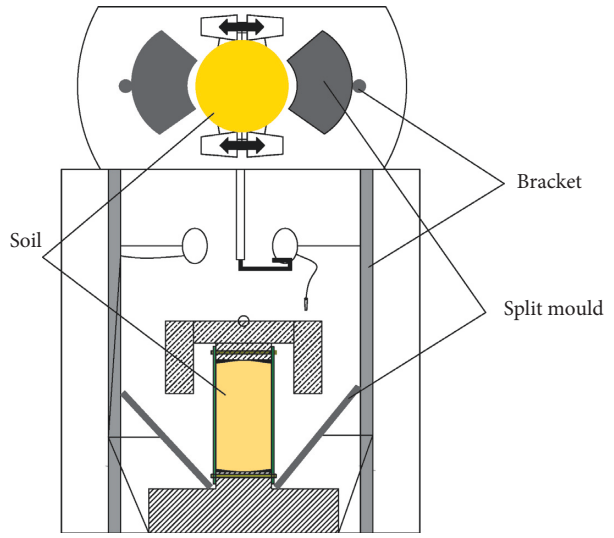

Figure 13: Schematic diagram of process ⑥.

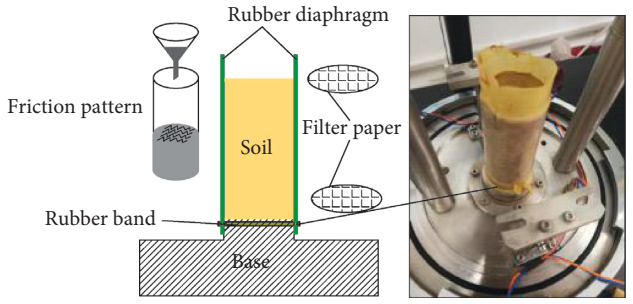

Figure 11: Schematic diagram of process ①.

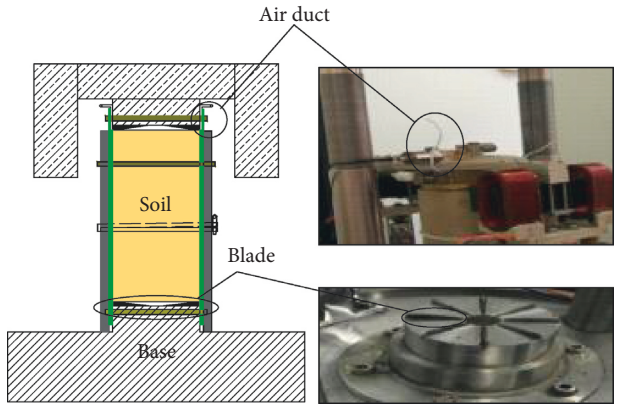

Figure 14: Schematic diagram of processes ③ and ④.

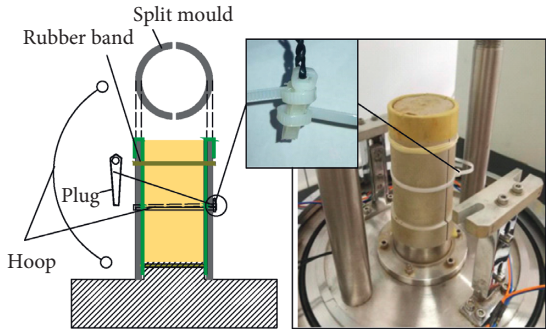

Figure 12: Schematic diagram of process ②.

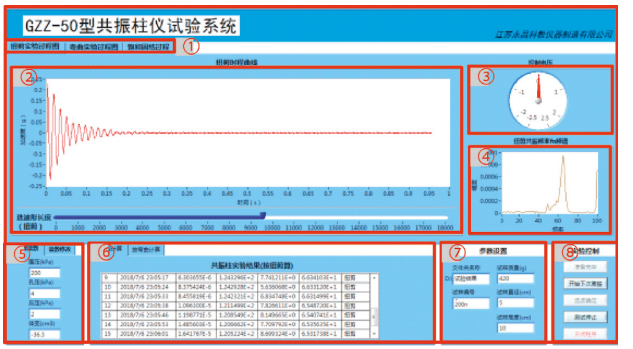

Figure 15: Functional division of free-vibration column of GZZ-50: ① test type, ② data records of accelerometer, ③ exciting force of drive board, ④ results of Fourier transform, ⑤ date records of other information, ⑥ results of test, ⑦ test parameters, and ⑧ test controller.

6. Testing Process and Data Deal

6.1. Testing Process. The functional division of free-vibration column of GZZ-50 is shown in Figure 15. The testing process of lateral vibration includes the following after installation:

① Enter some basic physical parameters of specimen, including diameter, height, and the weight

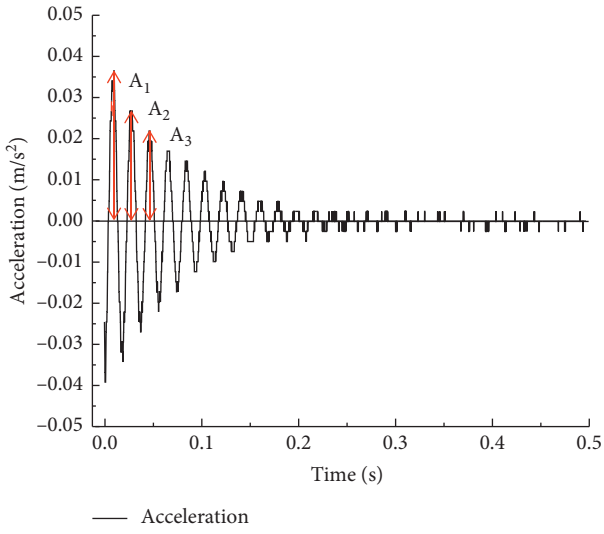

Figure 16: Curves of acceleration and time.

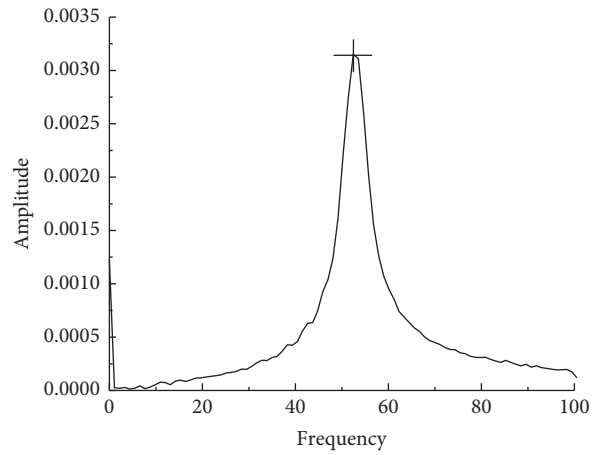

Figure 17: Curves of amplitude and frequency.

② Calculate z in numerical method according function 9

③ Start the lateral vibrating and record the data recorded by accelerometers

④ Calculate dynamic elastic modulus based on the natural frequency and count the damping ratio in logarithmic function according to the curves of acceleration along time

⑤ Increase amplitude of dynamic strain and repeat the above process till the tests are completed.

6.2. Deal with Obtained Data. The testing results of soil are shown in Figure 16. It can be found that the curves of testing results are not smooth, but the total tendency is clear. The greater measuring accuracy of accelerometer means many kinds of accelerate data will be recorded, which not only includes the natural accelerate of specimen but also includes the accelerate characteristic arisen from other situations, so the curves of accelerate is not single. The Fourier transform is a good solution for the problem [22]. The acceleration-time curves were transferred to amplitude-frequency curves (shown in Figure 17), and the natural frequency of specimen was obtained. Then, the dynamic elastic modulus of specimen will be obtained according to function 10, and the damping ratio will be obtained according to function 11:

$$\lambda = \frac{1}{2\pi}\frac{1}{m}\mathrm{In}\frac{A_n}{A_{n+m}}, \tag{11}$$

where A_n is the amplitude of nth peak and A_{n+m} is the amplitude of $(n+m)$'s peak.

7. Conclusion

Based on analysis of the lateral vibration theory of cantilever beam with an additional mass and descriptions about improved free-vibration column of GZZ-50, the following conclusions can be obtained:

(1) According to bending vibration equation of cantilever beam with additional mass, linking with free-vibration column of GZZ-50, a new testing method to measure dynamic elastic modulus of specimen was put forward

(2) Making descriptions about the calibration process of system parameters, and applying standard bars to confirm the calibration results

(3) 4 kinds of improvements of free-vibration column of GZZ-50 was proposed, including the adjustment of drive board shape, addition of hook with plug, laser displacement sensor uncontacted with specimen, and hollow duct, to improve the measured results or expand the testing scope of soil types

(4) The installation process of specimen and the deal process of data were described, which can be used as a reference of the similar instruments.

Appendix

The method improvements of testing modulus of soils in this paper were based on free-vibration column showed in Figure 1. This part is a simple introduction of the instrument. The free-vibration column was originally made by Nanjing University of Technology in China and improved by the authors of this paper, which had a higher measuring accuracy and a strain range within 10^{-6}–10^{-4}. The instrument consists of the following main components: (1) confining pressure-changing device and pressure chamber, (2) signal control device, (3) driving device in pressure chamber, (4) draining condition control device, (5) electrical signal enlarging device and acceleration acquisition device, and (6) data dealing device.

Data Availability

The data used to support the findings of this study are available from the corresponding author upon request.

Conflicts of Interest

The authors declare that they have no conflicts of interest.

Acknowledgments

The authors would like to thank the National Natural Science Foundation of China (grant nos. 51978317 and 51708256) for the support.

References

[1] E. E Eseller-Bayat, S. Gokyer, M. K. Yegian, R. O. Deniz, and A. Alshawabkeh, "Bender elements and bending disks for measurement of shear and compression wave velocities in large fully and partially saturated sand specimens," *Geotechnical Testing Journal*, vol. 36, no. 2, pp. 275–282, 2013.

[2] L. R. Hoyos, E. A. Suescún-Florez, and A. J. Puppala, "Stiffness of intermediate unsaturated soil from simultaneous suction-controlled resonant column and bender element testing," *Engineering Geology*, vol. 188, pp. 10–28, 2015.

[3] C. G. Xing, Z. D. Hua, and H. Q. Zhi, "Development and property test of gzz-1 free vibration column test system," *Earthquake Engineering and Engineering Vibration*, vol. 23, no. 1, pp. 110–114, 2003.

[4] D. Yang, "Investigation of the excess pore water pressure inside compacted asphalt mixture by dynamic triaxial tests," *Construction and Building Materials*, vol. 138, pp. 363–371, 2017.

[5] F. Zeng and L. Shao, "Unloading elastic behavior of sand in cyclic triaxial tests," *Geotechnical Testing Journal*, vol. 39, no. 3, pp. 462–475, 2016.

[6] S.-H. Chong and J.-Y. Kim, "Nonlinear vibration analysis of the resonant column test of granular materials," *Journal of Sound and Vibration*, vol. 393, pp. 216–228, 2017.

[7] H. Zhuang, R. Wang, G. Chen, Y. Miao, and K. Zhao, "Shear modulus reduction of saturated sand under large liquefaction-induced deformation in cyclic torsional shear tests," *Engineering Geology*, vol. 240, pp. 110–122, 2018.

[8] H. J. Mashhoud, J.-H. Yin, A. K. Panah, and Y. F. Leung, "Shaking table test study on dynamic behavior of micropiles in loose sand," *Soil Dynamics and Earthquake Engineering*, vol. 110, pp. 53–69, 2018.

[9] G.-X. Chen, B.-H. Wang, and T. Sun, "Dynamic shear modulus of saturated Nanjing fine sand in large scale shaking table tests," *Chinese Journal of Geotechnical Engineering*, vol. 34, no. 4, pp. 582–590, 2012.

[10] M. E. Kalinski and M. Thummaluru, "A new free-free resonant column device for measurement of gsub max and dsub min at higher confining stresses," *Geotechnical Testing Journal*, vol. 28, no. 2, pp. 180–187, 2005.

[11] F. Y. Menq, *Dynamic Properties of Sandy and Gravelly Soils*, University of Texas, Austin, TX, USA, 2003.

[12] J. U. Youn, Y. W. Choo, and D. S. Kim, "Measurement of small-strain shear modulus gmax of dry and saturated sands by bender element, resonant column, and torsional shear tests," *Revue Canadienne De Géotechnique*, vol. 45, no. 10, pp. 1426–1438, 2006.

[13] K. Senetakis and H. He, "Dynamic characterization of a biogenic sand with a resonant column of fixed-partly fixed boundary conditions," *Soil Dynamics and Earthquake Engineering*, vol. 95, pp. 180–187, 2017.

[14] Y.-X. Huang, H. Tian, and Y. Zhao, "Effects of cable on the dynamics of a cantilever beam with tip mass," *Shock and Vibration*, vol. 2016, Article ID 7698729, 10 pages, 2016.

[15] B. Lin, F. Zhang, D. Feng, K. Tang, and X. Feng, "Dynamic shear modulus and damping ratio of thawed saturated clay under long-term cyclic loading," *Cold Regions Science and Technology*, vol. 145, pp. 93–105, 2018.

[16] X.-z. Ling, Z.-y. Zhu, F. Zhang et al., "Dynamic elastic modulus for frozen soil from the embankment on Beiluhe Basin along the Qinghai-Tibet railway," *Cold Regions Science and Technology*, vol. 57, no. 1, pp. 7–12, 2009.

[17] G. Cascante, C. Santamarina, and N. Yassir, "Flexural excitation in a standard torsional-resonant column device," *Canadian Geotechnical Journal*, vol. 35, no. 3, pp. 478–490, 1998.

[18] B. N. Madhusudhan and K. Senetakis, "Evaluating use of resonant column in flexural mode for dynamic characterization of Bangalore sand," *Soils and Foundations*, vol. 56, no. 3, pp. 574–580, 2016.

[19] B. O. Hardin and V. P. Drnevich, "Shear modulus and damping in soil: measurement and parameter effects," *Asce Soil Mechanics and Foundation Division Journal*, vol. 98, no. 6, pp. 603–624, 1972.

[20] S. Rao, "Mechanical vibrations," *Nature*, vol. 179, no. 4558, p. 504, 2006.

[21] B. Wang, Z. Wang, and X. Zuo, "Frequency equation of flexural vibrating cantilever beam considering the rotary inertial moment of an attached mass," *Mathematical Problems in Engineering*, vol. 2017, no. 4, Article ID 1568019, 5 pages, 2017.

[22] M. Greenblatt, "Fourier transforms of irregular mixed homogeneous hypersurface measures," *Mathematische Nachrichten*, vol. 291, no. 7, pp. 1075–1087, 2018.